Molecular Pharmacology Fast Forward. Published on June 14, 2018 as DOI: 10.1124/mol.118.112177
This article has not been copyedited and formatted. The final version may differ from this version.

Title Page

Lipophilicity of the Cystic Fibrosis drug, ivacaftor (VX-770), and its destabilizing effect on the major CF-causing mutation: F508del.

Stephanie Chin, Maurita Hung, Amy Won, Yu-Sheng Wu, Saumel Ahmadi, Donghe Yang, Salma Elmallah, Krimo Toutah, C. Michael Hamilton, Robert N. Young, Russell D. Viirre, Christopher M. Yip, and Christine E. Bear

Department of Molecular Medicine (S.C., M.H., Y-S.W., S.A., D.Y., C.E.B.), Hospital for Sick Children, Toronto, Ontario, Canada; Department of Biochemistry (S.C., C.E.B.), Department of Physiology (M.H., Y-S.W., S.A., C.E.B.), Institute of Biomaterials and Biomedical Engineering (A.W., C.M.Y.), University of Toronto, Toronto, Ontario, Canada; Department of Chemistry and Biology (S.E., K.T., R.D.V.), Ryerson University, Toronto, Ontario, Canada; Department of Chemistry (C.M.H., R.N.Y.), Simon Fraser University, Burnaby, British Columbia, Canada

Molecular Pharmacology Fast Forward. Published on June 14, 2018 as DOI: 10.1124/mol.118.112177
This article has not been copyedited and formatted. The final version may differ from this version.

Running Title Page

Running title: The lipophilicity of VX-770 affects F508del-CFTR stability

Corresponding Author:
Dr. Christine E. Bear, Peter Gilgan Centre for Research and Learning, Department of Molecular Medicine, Hospital for Sick Children, 686 Bay Street, Room 209420 U-West, Toronto, ON, M5G 0A4, Phone: (416) 813-5981; Fax: (416) 813-5028; E-mail: bear@sickkids.ca

Text pages: 38

Tables: 0

Figures: 5

References: 60

Number of words:

Abstract: 250

Introduction: 711

Discussion: 1298

Nonstandard abbreviations: ABC (ATP-Binding Cassette), BMOE (bismaleimidoethane), CF (Cystic Fibrosis), CFTR (cystic fibrosis transmembrane conductance regulator), CH (coupling helix), Endoglycosidase (Endo), F508del (deletion of phenylalanine at position 508), HEK (human embryonic kidney), ICL (intracellular loop), log*P* (partition coefficient), MSD (membrane spanning domain), NBD (nucleotide binding domain), pTIRF (polarized total internal reflection fluorescence), R (regulatory), SLB (supported lipid bilayer), SLC (solute carrier), SM (sphingomyelin)

Molecular Pharmacology Fast Forward. Published on June 14, 2018 as DOI: 10.1124/mol.118.112177
This article has not been copyedited and formatted. The final version may differ from this version.

ABSTRACT

Deletion of phenylalanine at position 508 (F508del) in cystic fibrosis transmembrane conductance regulator (CFTR) is the most common Cystic Fibrosis (CF) causing mutation. Recently, ORKAMBI®, a combination therapy that includes a corrector of the processing defect of F508del-CFTR (lumacaftor or VX-809) and a potentiator of channel activity (ivacaftor or VX-770), was approved for CF patients homozygous for this mutation. However, clinical studies revealed that the effect of ORKAMBI® on lung function is modest and it was proposed that this modest effect relates to a negative impact of VX-770 on the stability of F508del-CFTR. In the current studies, we showed that this negative effect of VX-770 at 10 micromolar correlated with its inhibitory effect on VX-809 mediated correction of the interface between the second membrane spanning domain and the first nucleotide binding domain bearing F508del. Interestingly, we found that VX-770 exerted a similar negative effect on the stability of other membrane localized solute carriers (SLC26A3, SLC26A9 and SLC6A14), suggesting that this negative effect is not specific for F508del-CFTR. We determined that the relative destabilizing effect of a panel of VX-770 derivatives on F508del-CFTR correlated with their predicted lipophilicity. Polarized total internal reflection fluorescence microscopy on a supported lipid bilayer model shows that VX-770, and not its less lipophilic derivative, increased the fluidity of and reorganized the membrane. In summary, our findings show that there is a potential for non-specific effects of VX-770 on the lipid bilayer and suggest that this effect may account for its destabilizing effect on VX-809 rescued F508del-CFTR.

INTRODUCTION

Cystic fibrosis (CF) is caused by mutations of a unique ATP-Binding Cassette (ABC) anion channel, cystic fibrosis transmembrane conductance regulator (CFTR) (Cutting, 2015). CFTR has two nucleotide binding domains (NBDs), two membrane spanning domains (MSDs) and a regulatory (R) domain. In addition, the interface between the NBDs and MSDs consists of alpha-helical intracellular loops (ICLs) and coupling helices (CHs). The ICL: NBD1 interface is disrupted by the major CF causing mutation, deletion of phenylalanine at position 508 (F508del), thereby compromising assembly and function (Mendoza et al., 2012; Rabeh et al., 2012).

The first Food and Drug Administration-approved medicine to treat the underlying cause of CF is KALYDECO® (ivacaftor or VX-770), a potentiator that enhances channel gating of wildtype (Wt) CFTR and CFTR with certain gating mutations (i.e. glycine to aspartic acid at position 551 or G551D) at the cell surface by directly binding to the protein to prolong its open state in an ATP-independent manner (Eckford et al., 2012; Jih and Hwang, 2013; Van Goor et al., 2009). On the other hand, patch clamp studies by Jih and Hwang suggested that both ATP-dependent and ATP-independent CFTR channel gating are modified by VX-770 (Jih and Hwang, 2013). Recently, ORKAMBI®, a combination of VX-770 and a corrector compound known as lumacaftor (VX-809), was approved for use in patients who are homozygous for the major CF mutation, F508del. The corrector compound, VX-809, acts to partially rescue the defect in protein mistrafficking and misprocessing exhibited by F508del-CFTR to the cell surface (Van Goor et al., 2011), by repairing the aberrant ICL: NBD1 interfaces (Loo et al., 2013; Okiyoneda et al., 2013; Rabeh et al., 2012;

Ren et al., 2013). VX-770 acts on the VX-809 corrected F508del-CFTR to augment its activity (Eckford et al., 2012; Jih and Hwang, 2013; Van Goor et al., 2009; Van Goor et al., 2011).

Unfortunately, ORKAMBI® mediates modest and variable clinical responses (Boyle et al., 2014), prompting further discovery efforts for more efficacious corrector compounds. Certain *in vitro* findings suggest that the modest *in vivo* effect may reflect an adverse effect of VX-770 on the stability of the VX-809 corrected protein (Cholon et al., 2014; Matthes et al., 2016; Veit et al., 2014). Thus, the aim of the current studies was to interrogate the mechanism underlying this destabilizing effect of VX-770 on the major CF mutant, F508del. We also assessed the specificity of this destabilizing effect of VX-770 by studying its interaction with other membrane proteins (including SLC26A3, SLC26A9 and SLC6A14) as well as the lipid bilayer.

MATERIALS AND METHODS

Chronic treatment of F508del-CFTR with VX-770 and its analogs. Human Embryonic Kidney (HEK)-293 cells stably expressing F508del-CFTR (HEK F508del) were plated on 24 well plates (Sarstedt, Nümbrecht, Germany) and maintained in Dulbecco's Modified Eagle's Medium (DMEM, Wisent, St-Bruno, Quebec, Canada) supplemented with 10% Fetal Bovine Serum (FBS, Wisent, St-Bruno, Quebec, Canada), 1% non-essential amino acids (NEAA, Wisent, St-Bruno, Quebec, Canada), 0.6 mg/ml G418 sulfate (Wisent, St-Bruno, Quebec, Canada) and 5 μg/ml blasticidin (Wisent, St-Bruno, Quebec, Canada) at 37°C with 5% CO_2 overnight. For the initial chronic VX-770 studies, HEK F508del cells were pre-treated with VX-770 at a pharmacological concentration (0.1 μM) or at a supra-pharmacological concentration (10 μM) with 3 μM VX-809 (Selleck Chemicals, Houston, TX) in the previously described media at 37°C with 5% CO_2 for 48 h. For the studies with VX-770 and its derivatives, HEK F508del cells were pre-treated with VX-770 (Selleck Chemicals, Houston, TX) or its various derivatives (SE and KT compounds) synthesized in Dr. Russell Viirre's laboratory (Toronto, Ontario, Canada) (manuscript in preparation, refer to **Supplementary Figure 2** for chemical structures of VX-770 derivatives) at a pharmacological concentration (0.1 μM) or at a supra-pharmacological concentration (10 μM) in the previously described media at 27°C with 5% CO_2 for 24 h. The synthesis and characterization of the SE compounds in this paper has previously been described in detail (Elmallah, 2012). The synthesis and characterization the KT compounds employed the same methodology as (Elmallah, 2012) for the most part but also incorporated additional reaction steps previously published by the Verkman group for modification of the left hand side of the VX-770

molecule (Pedemonte et al., 2005).

Generation of mutants and constructs. The V510C, A1067C and V510C/A1067C cysteine-less (cys-less) variants of Wt-CFTR were kindly provided by Dr. David Clarke (Toronto, Ontario, Canada), the SLC26A3 and SLC26A9 constructs with N-terminal FLAG tags were kindly provided by Dr. Reinhart Reithmeier (Toronto, Ontario, Canada) and the SLC6A14 construct with a C-terminal FLAG tag was generated by OriGene (Rockville, MD). The F508del mutation was generated on the V510C/A1067C cys-less variant of Wt-CFTR background with primers (Forward: 5'-CATTAAAGAAAATATCATTGGTTGTTCCTATGATG-3' and Reverse: 5'-CATCATAGGAACAACCAATGATATTTTCTTTAATG-3') and the KAPA HiFi HotStart PCR Kit (KAPA Biosystems, Woburn, MA). Plasmid DNA was expanded with the QIAprep Spin Miniprep Kit (Qiagen, Hilden, Germany) and the sequence was confirmed with DNA sequencing (TCAG, Toronto, Ontario, Canada). HEK-293 GripTite (GT) cells, kindly provided by Dr. Daniella Rotin's laboratory (Toronto, Ontario, Canada), were maintained in DMEM (Wisent, St-Bruno, Quebec, Canada) supplemented with 10% FBS (Wisent, St-Bruno, Quebec, Canada), 1% NEAA (Wisent, St-Bruno, Quebec, Canada) and 0.6 mg/ml G418 sulfate (Wisent, St-Bruno, Quebec, Canada), transfected with constructs using PolyFect Transfection Reagent (Qiagen, Hilden, Germany) according to the manufacturer's protocol and temperature rescued at 27°C with 5% CO_2 for 24 h.

Cysteine cross-linking. HEK-293 GT cells were grown on 24 well plates (Sarstedt, Nümbrecht, Germany) at 37°C with 5% CO_2 overnight and then transfected with cys-less variants of CFTR. Cells were treated with DMSO (0.1%), VX-809 (3 μM), VX-770 (0.1 or 10 μM), or VX-809 plus

VX-770 (0.1 or 10 μM) at 27°C with 5% CO_2 for 24 h. The next day, cells were treated with 50 μM bismaleimidoethane (BMOE, Life Technologies, Rockford, IL) in DMEM (Wisent, St-Bruno, Quebec, Canada) supplemented with 10% FBS (Wisent, St-Bruno, Quebec, Canada), 1% NEAA (Wisent, St-Bruno, Quebec, Canada) and 0.6 mg/ml G418 sulfate (Wisent, St-Bruno, Quebec, Canada) at 27°C with 5% CO_2 for 1 h.

Deglycosylation studies. Cys-less variants of CFTR were lysed from HEK-293 GT cells into radioimmunoprecipitation assay (RIPA; 50 mM Tris-Base, 150 mM sodium chloride, 1 mM EDTA, 1% (v/v) Triton X-100, 0.1% (v/v) SDS, 1X protease inhibitor cocktail (AMRESCO, Cleveland, OH), pH 7.4) buffer. Protein samples were treated with Endoglycosidase H and PNGase F according to the manufacturer's protocol (New England Biolabs, Ipswich, MA).

Chronic treatment of SLC proteins with VX-770. HEK-293 GT cells were grown on 24 well plates (Sarstedt, Nümbrecht, Germany) at 37°C with 5% CO_2 overnight and transfected with the SLC constructs. Cells were then treated with various concentrations of VX-770 (0, 0.1, 1, 2, 10 μM) at 27°C with 5% CO_2 for 24 h.

Immunoblotting. HEK F508del and HEK-293 GT cells were lysed into RIPA buffer and protein samples were subjected to SDS-PAGE. CFTR protein samples were run on 6% Tris-Glycine sodium dodecyl sulfate (TG SDS) gels (Life Technologies, Carlsbad, CA) and SLC protein samples were run on 8% TG SDS gels (Life Technologies, Carlsbad, CA). Protein samples were transferred to nitrocellulose paper and probed with the following primary antibodies overnight at 4°C shaking: IgG2b mAb596 antibody (University of North Carolina at Chapel Hill, Chapel Hill,

NC, code: A4, Cystic Fibrosis Foundation Therapeutics Inc.) for CFTR protein (1:5000 for F508del-CFTR, 1:1000 for V510C/A1067C cys-less variant of Wt-CFTR, 1:500 for V510C/A1067C cys-less variant of F508del-CFTR), calnexin-specific rabbit pAb (1:10000, Sigma-Aldrich, St. Louis, MO, cat. no.: C4731) for calnexin loading control, anti-mouse FLAG antibody (Sigma-Aldrich, St. Louis, MO, 1:2500) for SLC protein, and anti-β-actin (1:10000, Abcam, Cambridge, UK, ab8229) for actin loading control. The samples were then probed with secondary antibodies for 1 h at room temperature shaking at concentrations twice as diluted as the primary antibodies as follows: horseradish peroxidase-conjugated goat anti-mouse IgG secondary antibody (Pierce, Rockford, IL) for CFTR protein and actin loading control, horseradish peroxidase–conjugated goat anti-rabbit IgG secondary antibody (Pierce, Rockford, IL) for calnexin loading control, and anti-mouse HA (Covance, Princeton, NJ, MMS-101R) for SLC protein. Westerns were exposed using Amersham enhanced chemiluminescent reagent (GE Healthcare Life Sciences, Mississauga, Ontario, Canada) with the Li-Cor Odyssey Fc (LI-COR Biosciences, Lincoln, NE) at a linear range of exposure. Densitometry of immunoblot bands were analyzed with Image Studio Lite software (Version 5.2.5) from Li-Cor Odyssey Fc (LI-COR Biosciences, Lincoln, NE).

FLiPR membrane potential assay. The FLiPR membrane potential assay was conducted as previously described (Molinski et al., 2015). Briefly, HEK F508del cells were grown on black 96 well plates with clear bottoms (Corning, Corning, NY) at 37°C with 5% CO_2 overnight. Cells were then treated with 3 μM VX-809 at 37°C with 5% CO_2 for 48 h. The next day, cells were loaded with 0.5 mg/ml FLiPR membrane potential dye (Molecular Devices, Sunnyvale, CA) in sodium gluconate buffer as previously described (Molinski et al., 2015) for 45 min with 5% CO_2 at 37°C.

Molecular Pharmacology Fast Forward. Published on June 14, 2018 as DOI: 10.1124/mol.118.112177
This article has not been copyedited and formatted. The final version may differ from this version.

Fluorescence was read at excitation of 530 nm and emission of 560 nm on the SpectraMax i3X fluorescence plate reader at 37°C (Molecular Devices, Sunnyvale, CA). Baseline fluorescence was read for 5 min. CFTR was stimulated by vehicle, 1 μM forskolin (Fsk, Sigma-Aldrich, St. Louis, MO), 1 μM Fsk with VX-770 (10 μM), or 1 μM Fsk with the derivative SE-03 (10 μM) for 10 min. CFTR was then inhibited with 10 μM CFTR inhibitor-172 ($CFTR_{inh}$-172, Cystic Fibrosis Foundation Therapeutics Inc. and Rosalind Franklin University of Medicine and Science, Chicago, IL) for 12 min. Curves were normalized to last point of baseline and the maximal points of stimulation were plotted with GraphPad Prism v6.01 (San Diego, CA).

Polarized Total Internal Reflection Fluorescence (pTIRF) Microscopy. The formation of supported lipid bilayers of 1:1:1 dioleoylphosphatidylcholine/egg sphingomyelin/cholesterol (DOPC/bSM/chol) and 1:1:1 DOPC/distearoylphosphatidylcholine/chol (DOPC/DSPC/chol) with $DilC_{18}$(3) (1 mol %, Life Technologies, Carlsbad, CA) in buffer (10 mM HEPES, 150 mM NaCl, pH 7.4) were prepared as previously described (Walsh et al., 2014). All images were acquired using a home-built pTIRF system incorporating four excitation laser lines built on an Olympus IX70 inverted microscope. All images were captured at 15 s intervals for 1 h with a water-cooled Evolve 512 EMCCD camera (Photometrics, Tucson, AZ) controlled by μ-Manager (http://www.micro-manager.org). Fluorescent probes were excited by substrate parallel (F*s*, *s*-polarized) and perpendicular (F*p*, *p*-polarized) polarized excitation at 532 nm through a half-wave liquid crystal variable retarder (LCC25 1111A, Thorlabs, Newton, NJ). Two bilayer studies were performed with multiple fields of view examined for each bilayer (3-6 fields). Order parameter $\langle P_2 \rangle$ values were determined for each region of interest and calculated on a per pixel basis using

an in-house macro. Refer to previous publications for more details (Oreopoulos et al., 2010; Oreopoulos and Yip, 2009).

Statistical analyses. Results were plotted and analyzed on GraphPad Prism v6.01 (San Diego, CA). Results were presented as mean ± SD with each replicate representing one biological replicate from an individual experiment. For all statistical analyses, One-way ANOVA and Dunnett's post-hoc test were conducted on GraphPad Prism v6.01 (San Diego, CA) for multiple comparisons of conditions to the control. The p-values were automatically adjusted by GraphPad Prism v6.01 (San Diego, CA) for the multiple comparisons and $p < 0.05$ was considered significantly different from the control.

RESULTS

Destabilizing effect of long-term treatment with micromolar concentrations of VX-770 on the abundance of VX-809 corrected F508del-CFTR protein. As previously reported (Cholon et al., 2014; Matthes et al., 2016; Veit et al., 2014), we observed a destabilizing effect of long-term (48 hours) treatment of VX-770 at a high concentration (10 μM) at 37°C on the relative abundance of the mature band *C* (**Figure 1B**) and immature band *B* (**Figure 1C**) forms of the VX-809 rescued F508del-CFTR protein in the HEK-293 expression system. As previously reported (Cholon et al., 2014), this was not related to a significant decrease in cell viability, with comparable abundance of calnexin (CNX) expression across the treatments (**Figure 1A**).

Micromolar VX-770 reverses the effect of VX-809 in stabilizing the ICL4: NBD1 interface of cys-less variant of F508del-CFTR. We were prompted to determine if this destabilizing effect of VX-770 was due in part, to a reversal of the positive effect of VX-809 on F508del-CFTR assembly. The corrector, VX-809, is thought to act by stabilizing the aberrant interaction between F508del in NBD1 and the intracellular loop ICL4 (conferred by MSD2) (Okiyoneda et al., 2013; Rabeh et al., 2012). As in previous publications (Aleksandrov et al., 2010; Chin et al., 2017; He et al., 2008; Loo et al., 2008; Loo and Clarke, 2011; Serohijos et al., 2008), we assessed this interaction by studying the propensity for chemical cross-linking between cysteine residues engineered at V510 (NBD1) and A1067 (ICL4) in the context of a full-length cysteine-less (cys-less) variant of CFTR protein for both Wt and F508del. The following studies were performed at 27°C as the cys-less variant of CFTR protein is misprocessed at 37°C and requires temperature rescue at 27°C to promote its maturation (He et al., 2008; He et al., 2013; Loo and Clarke, 2006; Wang et al., 2007).

Molecular Pharmacology Fast Forward. Published on June 14, 2018 as DOI: 10.1124/mol.118.112177
This article has not been copyedited and formatted. The final version may differ from this version.

The V510C/A1067C cys-less variant of Wt-CFTR runs as two bands: the mature, complex glycosylated band *C* and the immature, core glycosylated band *B* (**Figure 2A**). As previously reported, band *C* is insensitive to Endoglycosidase (Endo) H, whereas band *B* is deglycosylated and this form is labeled as band *A*. Both band *B* and *C* are deglycosylated by PNGase F as shown on the left panels of **Figure 2A**. We confirmed that two cysteine residues (V510C on NBD1 and A1067C on ICL4) could be cross-linked by a cell-permeable maleimide reagent, bismaleimidoethane (BMOE), in a V510C/A1067C cys-less variant of Wt-CFTR protein with the appearance of a cross-linked species (ŧ) that migrates as a 250 kDa protein on a SDS-PAGE gel (**Figure 2A**) (Chin et al., 2017). We confirmed that this band (ŧ) was conferred by intramolecular rather than intermolecular cross-linking as it was not produced when single cysteine containing constructs (V510C or A1067C) were expressed alone or together (**Supplementary Figure 1**) (Chin et al., 2017). We showed that the band (ŧ) is Endo H resistant and hence, complex glycosylated. Interestingly, an N-glycanase resistant band (△) was apparent in the cross-linker treated cells but not in the absence of cross-linker (**Figure 2A** and **Supplementary Figure 1**). We suggest on the basis of its glycosidase resistance, that this unique band is the cross-linked form of band *A*.

A V510C/A1067C cys-less variant of F508del-CFTR is misprocessed with no appearance of band *C* in SDS-PAGE, with just the misprocessed band *B* expressed (**Figure 2A**) (Loo et al., 2008; Loo and Clarke, 2011). Treatment with the cell-permeable cross-linker (BMOE) led to the appearance

Molecular Pharmacology Fast Forward. Published on June 14, 2018 as DOI: 10.1124/mol.118.112177
This article has not been copyedited and formatted. The final version may differ from this version.

of a unique band (❋). This band (❋) shifted slightly following Endo H treatment to (△), confirming that it is not the *C* band, but rather the cross-linked band *B*. The band (△) of this mutant protein is N-glycanase resistant, suggesting that it represents the cross-linked band *A*.

Long term (24 hours) treatment of V510C/A1067C cys-less variant of F508del-CFTR with VX-809 (3 μM) did not lead to its maturation and the appearance of band *C*, likely due to the number of mutations introduced to eliminate endogenous cysteines (**Figure 2B**). However, this treatment did lead to a significant increase in the cross-linking between V510C and A1067C with an increased ratio of the cross-linked band *B* (❋) relative to band *B* (**Figure 2B and 2C**). These findings are consistent with previous studies, showing its positive effect in improving interaction between NBD1 and ICL4 (Loo et al., 2013; Ren et al., 2013; Van Goor et al., 2011). This positive effect of VX-809 was reversed when VX-770 (10 μM) was included in this long-term treatment (**Figure 2B and 2C**). This abolition of NBD1: ICL4 assembly following the combination treatment could explain the effect observed on processing as documented in **Figure 1**. As in the case of the protein processing studies shown in **Figure 1**, the destabilizing effect of VX-770 on domain: domain assembly is dose-dependent and no destabilizing effect on cross-linking was observed following co-treatment with VX-770 at 0.1 μM (**Figure 2B and 2C**).

Micromolar concentrations of VX-770 also exert a destabilizing impact on other membrane proteins. We were interested to determine if the destabilizing effect of 10 μM VX-770 was specific to F508del-CFTR. In order to maintain similar conditions to our cysteine cross-linking studies, we tested its specificity by applying this concentration of VX-770 at 27°C on HEK-293 cells

expressing other membrane proteins, including solute carriers (SLCs): SLC26A3, SLC26A9 and SLC6A14. These membrane proteins are particularly important as they have been shown to interact with and/or modify CFTR channel activity in various epithelial tissues (Anagnostopoulou et al., 2012; Avella et al., 2011; Bertrand et al., 2009; Chang et al., 2009; Gupta et al., 2006; Karunakaran et al., 2011; Ko et al., 2004; Xu et al., 2005). Further, these SLC genes have been shown to modify CF disease phenotypes (Corvol et al., 2015; Li et al., 2014b; Strug et al., 2016; Sun et al., 2012). Thus, we reason that it would be disadvantageous for CFTR modulatory drugs to also affect the expression of these membrane proteins.

Firstly, analysis of the SLC proteins by SDS-PAGE revealed multiple glycosylation states as previously reported (Li et al., 2014a). Interestingly, the steady state abundance of all the SLCs in this study was significantly decreased with chronic treatment with micromolar concentrations of VX-770 at 27°C (**Figure 3**). SLC26A3 appeared to be the most susceptible to VX-770 as its protein expression significantly decreased at concentrations of VX-770 as low as 0.1 μM (**Figure 3A**). On the other hand, the abundance of SLC26A9 and SLC6A14 was significantly decreased starting at higher concentrations of 2 μM and 10 μM VX-770 respectively (**Figure 3B and 3C**). Therefore, the destabilizing effect of supra-pharmacological concentrations of VX-770 is not specific to F508del-CFTR.

Lipophilicity of VX-770 appears to be correlated with the destabilizing effect on F508del-CFTR.

We propose that the non-specific, destabilizing effects of supra-pharmacological concentrations of VX-770 may be related to the known effects of this compound on the lipid bilayer (Baroni et al., 2014). To test this idea, VX-770 derivatives (**Supplementary Figure 2**) with varying degrees

Molecular Pharmacology Fast Forward. Published on June 14, 2018 as DOI: 10.1124/mol.118.112177
This article has not been copyedited and formatted. The final version may differ from this version.

of lipophilicity, as assessed by their partition coefficient (log*P*) values, were incubated with HEK-293 cells expressing temperature–rescued F508del-CFTR and their effects on the processing (band *C/C+B*) of F508del-CFTR determined.

In this study, the HEK-293 cells expressing F508del-CFTR were treated with VX-770 or a derivative for 24 hours at 0.1 or 10 μM at 27°C. We observed a negative correlation between the lipophilicity or log*P* values and the relative band *C/C+B* ratio (**Figure 4B**). Derivatives with low log*P* scores (i.e. SE-02, SE-03, KT-226 and KT-227) were associated with a higher band *C/C+B* ratio than the derivatives with high log*P* scores (i.e. KT-51, KT-126, KT-127 and KT-128) (**Figure 4A and 4B**). For example, the derivative SE-03, while exhibiting potentiator activity (**Figure 4D and 4E**), did not reduce steady state protein abundance at 10 μM (**Figure 4C**).

Micromolar concentrations of VX-770 increase the membrane fluidity in a lipid raft model. Given the potential role for lipophilicity in VX-770 dependent effects on membrane protein stability, we were prompted to determine if the non-specific destabilizing effects of micromolar concentrations of VX-770 were mediated by disrupting lipid rafts. We tested this hypothesis using a synthetic lipid raft model and tested the effect of micromolar VX-770 on membrane fluidity and bilayer integrity. Polarized total internal reflection fluorescence (pTIRF) microscopy was employed to study the effect of 10 μM VX-770 on a supported lipid bilayers (SLB) that contained DOPC/cholesterol/DSPC and DOPC/cholesterol/sphingomyelin (bSM) bathed in a HEPES buffer (Calder and Yaqoob, 2007; Simons and Toomre, 2000). Two distinct bilayers were tested for the effect of VX-770 with 3-6 fields of view analyzed per bilayer (**Figure 5A and 5B**). Order parameter $\langle P_2 \rangle$ measurements and the histogram movies demonstrated that 10 μM VX-770 immediately increased

the bilayer fluidity as well as reorganized subdomains within the DOPC/bSM/cholesterol SLB. The histograms were determined from the selected field of view and that same field of view was used to track the dynamic changes in the bilayer upon VX-770 addition. As such, our interpretations as to the effect of these agents on membrane stability and structure are drawn from relative changes in the individual histogram characteristics for the chosen field of view. From that perspective, we can clearly see that there is a clear shift to a higher mean $<P_2>$ value and a tighter distribution upon VX-770, which is strongly suggestive of increased membrane fluidity. This interpretation is certainly bolstered by the before- and after-VX-770 addition, which shows significant changes in the bilayer domain structures. Conversely, the relative decrease and broadening of the distribution of $<P_2>$ values (i.e. emergence of a second lower $<P_2>$ peak) upon SE-03 addition can only be interpreted at this point as evidence of a greater extent of membrane reorganization. Intriguingly, the extent of sub-domain restructuring due to SE-03 addition appears to be significantly less than in the VX-770 case, as is evidenced by the relatively minor changes in bilayer morphology (**Figure 5C and 5D**), supporting the claim the VX-770 effects are mediated at least in part by its relative lipophilicity.

Molecular Pharmacology Fast Forward. Published on June 14, 2018 as DOI: 10.1124/mol.118.112177
This article has not been copyedited and formatted. The final version may differ from this version.

DISCUSSION

The current studies provide a potential explanation for the concentration-dependent, destabilizing effects of chronic exposure to VX-770 on VX-809 rescued F508del-CFTR protein (Cholon et al., 2014; Matthes et al., 2016; Veit et al., 2014). At the concentrations of VX-770 that reduce F508del-CFTR protein stability, we also observed reduction of the abundance of other membrane proteins (SLC26A3, SLC26A9 and SLC6A14) pointing to its lack of specificity. From our studies of model lipid rafts, we deduce that this negative effect of high concentrations of VX-770 is related to its lipophilicity and disruption of these membrane structures.

Our biochemical studies showed that the concentration of VX-770 (10 μM) that reduced VX-809-mediated augmentation in F508del-CFTR processing also reversed VX-809 mediated enhancement of the interaction between the intracellular loop conferred by MSD2 (ICL4) and NBD1. As in previous studies (Aleksandrov et al., 2010; Chin et al., 2017; He et al., 2008; Loo et al., 2008; Loo and Clarke, 2011; Serohijos et al., 2008), we probed the interaction at this interface in the context of a cys-less variant of F508del-CFTR protein harbouring cysteine residues engineered in ICL4 (A1067C) and NBD1 (V510C). In our experimental system, we could not detect VX-809 induced maturation and processing of the V510C/A1067C cys-less variant of F508del-CFTR protein in immunoblots. However, VX-809 induced interface assembly in the immature, core-glycosylated band *B* of the protein was detectable as a unique cross-linked band (✳) and the relative abundance of this band was reduced in the presence of 10 μM VX-770 but not in the presence of 100 nM VX-770. Hence, we interpret the destabilizing effects of VX-770 at this

concentration to be due to inhibition of the positive effects of VX-809 at this interface. However, as discussed in the subsequent paragraphs, this effect is likely not specific to this interface or even the mutant CFTR protein.

The same concentration of VX-770 that induced destabilizing effects on F508del-CFTR assembly also reduced the steady state abundance of the three SLC proteins tested. We chose these proteins because they are known to be localized in the same tissues and membranes as CFTR and modify epithelial transport function (Ko et al., 2004; Mount and Romero, 2004; Sun et al., 2012). Hence, any non-specific effect of VX-770 on these membrane proteins may have a potential to modify disease and/or therapeutic response to ORKAMBI®. Of these proteins, SLC26A3 was the most sensitive to the destabilizing effect of VX-770, with a significant decrease in protein abundance apparent (at least in the HEK-293 expression system) at 1 μM, the serum concentration reported by Vertex Pharmaceuticals (Vertex Pharmaceuticals Incorporated, 2017). Previous studies have shown that loss of function mutations of SLC26A3 caused a rare disease known as congenital chloride-losing diarrhea via impaired chloride absorption and fluid/bicarbonate secretion (Hoglund et al., 1996). Intestinal inflammation, which is common in diarrhea, has been found to further reduce SLC26A3 expression through direct binding to NF-kB (Kumar et al., 2017). Hence, it is possible that the destabilizing effect of VX-770 that we observed on SLC26A3 may modify the ORKAMBI® response in the intestinal tissues.

SLC26A9 confers an apical anion channel and this function augments the cAMP-regulated channel activity of CFTR in the non-CF airway epithelium and in the epithelium of patients bearing gating mutations such as G551D (Bertrand et al., 2017; Bertrand et al., 2009). Strug et al. showed that

polymorphisms in the *SLC26A9* gene associate with the response of patients bearing G551D to VX-770 and interpreted these results to suggest that functional expression of SLC26A9 enhances the therapeutic efficacy of VX-770 in this cohort of patients (Strug et al., 2016). Therefore, VX-770 in patient tissues is not impairing the positive affect of SLC26A9 on the potentiation of the G551D channel. On the other hand, the misfolded F508del-CFTR protein interacts with and prevents SLC26A9 trafficking to the apical surface (Bertrand et al., 2017; Bertrand et al., 2009). Correction of F508del-CFTR by VX-809, is thought to promote SLC26A9 trafficking to the cell surface indirectly (Bertrand et al., 2017; Bertrand et al., 2009). *In vitro* studies of bronchial explant tissue from F508del homozygotes suggest that the magnitude of pharmacological correction by VX-809 is also augmented by SLC26A9 expression (Strug et al., 2016). Hence, the results of the current study suggest that the possible deleterious effect of chronic VX-770 on SLC26A9 protein stability should be further studied given its importance in modifying the pharmacological rescue conferred by this therapy.

SLC6A14 is an apical amino acid transporter and we have shown that it functions to remove nutrient amino acids from the surface of respiratory epithelial cells (Di Paola et al., 2017). This function is associated with reduced adherence of *Pseudomonas aeruginosa* to the surface of respiratory epithelial cells (Di Paola et al., 2017). We speculate that reduced surface stability of SLC6A14 induced by high concentrations of VX-770 would potentially enhance *P. aeruginosa* attachment and biofilm formation and we are testing this hypothesis.

We propose that the destabilizing effect of VX-770 is related to its lipophilic property. Interestingly, treatment of F508del-CFTR with a panel of VX-770 derivatives showed that the

degree of VX-770 lipophilicity is correlated to its destabilizing effect. SE-03 lacks two tert-butyl groups on the phenol ring (**Supplementary Figure 2**) and is less lipophilic than VX-770 (the log*P* value of SE-03 is 2.67 whereas it is 5.76 for VX-770), yet it retains activity as a potentiator. Interestingly, SE-03 does not reduce F508del-CFTR protein stability even at the high concentration of 10 μM. Biophysical studies of a lipid raft model showed that unlike VX-770, SE-03 addition did not disperse lipid rafts comprised of cholesterol and sphingomyelin. Together, these findings support the hypothesis that the non-specific effects of VX-770 on membrane protein stability are mediated through VX-770 interaction with and disruption of lipid rafts, a membrane organizing structure known to facilitate protein interactions and signaling (Abu-Arish et al., 2015; Bi et al., 2001; Patel et al., 2008; Steinberg, 2008).

The non-specific effect of chronic VX-770 on the steady state abundance of F508del-CFTR, other membrane proteins and lipid rafts was observed at the supra-pharmacological concentration of 10 μM VX-770. According to Matthes et al., a peak free plasma concentration of VX-770 is 1.5-8.5 nM, considerably lower than other estimates and the concentration at which we observed the non-specific effects of VX-770 (Hanrahan et al., 2017; Matthes et al., 2016). According to the drug data sheet provided by Vertex, after a single recommended dose of 150 mg administered after a meal, the peak plasma concentration reaches 768 ng/ml or 1-2 μM (Vertex Pharmaceuticals Incorporated, 2017). This value is an order of magnitude less than the concentration (10 μM) that caused significant loss of CFTR and other membrane proteins (including SLC26A9) in the *in vitro* studies of this paper. However, according to a previous study (Trittler and Hug, 2014), there was a large range in serum concentrations of VX-770 in different patients, ranging from 400-3000 ng/ml, with the upper limit approaching 10 μM. Importantly, the concentration of VX-770 in the

tissues of CF patients treated with VX-770 is uncertain. According to the European Medicine Agency (EMA/473279/2012), VX-770 accumulates in lung and tracheal epithelial tissues relative to plasma in rat studies (European Medicine Agency, 2012). Hence, it remains unknown if tissue concentrations could approach the higher concentration of 10 μM shown to exert non-specific, destabilizing effects.

It is important to acknowledge that VX-770 exerts a beneficial effect overall when given as a monotherapy to individuals bearing gating mutations in CFTR. However, our studies suggest that future clinical studies are required to monitor off-target effects in this population taking this monotherapy continuously over their lifetime. Finally, it remains possible that the variable clinical efficacy of ORKAMBI® in the F508del patient population is partially associated with variation in its tissue accumulation amongst patients and/or off-target effects of VX-770 on other membrane proteins variably expressed in different patients.

Molecular Pharmacology Fast Forward. Published on June 14, 2018 as DOI: 10.1124/mol.118.112177
This article has not been copyedited and formatted. The final version may differ from this version.

ACKNOWLEDGEMENTS

We would like to thank Dr. David Clarke for providing the V510C, A1067C and V510C/A1067C cys-less variants of Wt-CFTR. We would like to thank Dr. Reinhart Reithmeier and OriGene for providing the SLC constructs. We would like to thank Dr. Steven Molinski for the helpful discussions on these studies. We would also like to thank Dr. Jacqueline McCormack for her help in editing the manuscript.

Molecular Pharmacology Fast Forward. Published on June 14, 2018 as DOI: 10.1124/mol.118.112177
This article has not been copyedited and formatted. The final version may differ from this version.

AUTHOR CONTRIBUTIONS

Participated in research design: Chin, Hung, Won, Wu, Yip, Bear

Conducted experiments: Chin, Hung, Won, Wu

Contributed new reagents or analytic tools: Ahmadi, Yang, Elmallah, Toutah, Hamilton, Young, Viirre, Yip

Performed data analysis: Chin, Hung, Won, Wu, Bear

Wrote or contributed to the writing of the manuscript: Chin, Hung, Won, Young, Viirre, Yip, Bear

REFERENCES

Abu-Arish A, Pandzic E, Goepp J, Matthes E, Hanrahan JW and Wiseman PW (2015) Cholesterol modulates CFTR confinement in the plasma membrane of primary epithelial cells. *Biophys J* **109**(1): 85-94.

Aleksandrov AA, Kota P, Aleksandrov LA, He L, Jensen T, Cui L, Gentzsch M, Dokholyan NV and Riordan JR (2010) Regulatory insertion removal restores maturation, stability and function of DeltaF508 CFTR. *J Mol Biol* **401**(2): 194-210.

Anagnostopoulou P, Riederer B, Duerr J, Michel S, Binia A, Agrawal R, Liu X, Kalitzki K, Xiao F, Chen M, Schatterny J, Hartmann D, Thum T, Kabesch M, Soleimani M, Seidler U and Mall MA (2012) SLC26A9-mediated chloride secretion prevents mucus obstruction in airway inflammation. *J Clin Invest* **122**(10): 3629-3634.

Avella M, Loriol C, Boulukos K, Borgese F and Ehrenfeld J (2011) SLC26A9 stimulates CFTR expression and function in human bronchial cell lines. *J Cell Physiol* **226**(1): 212-223.

Baroni D, Zegarra-Moran O, Svensson A and Moran O (2014) Direct interaction of a CFTR potentiator and a CFTR corrector with phospholipid bilayers. *Eur Biophys J* **43**(6-7): 341-346.

Bertrand CA, Mitra S, Mishra SK, Wang X, Zhao Y, Pilewski JM, Madden DR and Frizzell RA (2017) The CFTR trafficking mutation F508del inhibits the constitutive activity of SLC26A9. *Am J Physiol Lung Cell Mol Physiol* **312**(6): L912-l925.

Bertrand CA, Zhang R, Pilewski JM and Frizzell RA (2009) SLC26A9 is a constitutively active, CFTR-regulated anion conductance in human bronchial epithelia. *J Gen Physiol* **133**(4): 421-438.

Bi K, Tanaka Y, Coudronniere N, Sugie K, Hong S, van Stipdonk MJ and Altman A (2001) Antigen-induced translocation of PKC-theta to membrane rafts is required for T cell activation. *Nat Immunol* **2**(6): 556-563.

Boyle MP, Bell SC, Konstan MW, McColley SA, Rowe SM, Rietschel E, Huang X, Waltz D, Patel NR and Rodman D (2014) A CFTR corrector (lumacaftor) and a CFTR potentiator (ivacaftor) for treatment of patients with cystic fibrosis who have a phe508del CFTR mutation: a phase 2 randomised controlled trial. *Lancet Respir Med* **2**(7): 527-538.

Calder PC and Yaqoob P (2007) Lipid rafts--composition, characterization, and controversies. *J Nutr* **137**(3): 545-547.

Chang MH, Plata C, Sindic A, Ranatunga WK, Chen AP, Zandi-Nejad K, Chan KW, Thompson J, Mount DB and Romero MF (2009) Slc26a9 is inhibited by the R-region of the cystic fibrosis transmembrane conductance regulator via the STAS domain. *J Biol Chem* **284**(41): 28306-28318.

Chin S, Yang D, Miles AJ, Eckford PD, Molinski S, Wallace BA and Bear CE (2017) Attenuation of Phosphorylation-dependent Activation of Cystic Fibrosis Transmembrane Conductance Regulator (CFTR) by Disease-causing Mutations at the Transmission Interface. *J Biol Chem* **292**(5): 1988-1999.

Cholon DM, Quinney NL, Fulcher ML, Esther CR, Jr., Das J, Dokholyan NV, Randell SH, Boucher RC and Gentzsch M (2014) Potentiator ivacaftor abrogates pharmacological correction of DeltaF508 CFTR in cystic fibrosis. *Sci Transl Med* **6**(246): 246ra296.

Corvol H, Blackman SM, Boelle PY, Gallins PJ, Pace RG, Stonebraker JR, Accurso FJ, Clement A, Collaco JM, Dang H, Dang AT, Franca A, Gong J, Guillot L, Keenan K, Li W, Lin F, Patrone MV, Raraigh KS, Sun L, Zhou YH, O'Neal WK, Sontag MK, Levy H, Durie PR, Rommens JM, Drumm ML, Wright FA, Strug LJ, Cutting GR and Knowles MR (2015) Genome-wide association meta-analysis identifies five modifier loci of lung disease severity in cystic fibrosis. *Nat Commun* **6**: 8382.

Cutting GR (2015) Cystic fibrosis genetics: from molecular understanding to clinical application. *Nat Rev Genet* **16**(1): 45-56.

Di Paola M, Park AJ, Ahmadi S, Roach EJ, Wu YS, Struder-Kypke M, Lam JS, Bear CE and Khursigara CM (2017) SLC6A14 Is a Genetic Modifier of Cystic Fibrosis That Regulates Pseudomonas aeruginosa Attachment to Human Bronchial Epithelial Cells. *MBio* **8**(6).

Eckford PD, Li C, Ramjeesingh M and Bear CE (2012) Cystic fibrosis transmembrane conductance regulator (CFTR) potentiator VX-770 (ivacaftor) opens the defective channel gate of mutant CFTR in a phosphorylation-dependent but ATP-independent manner. *J Biol Chem* **287**(44): 36639-36649.

Elmallah (2012) Progress toward the synthesis of labeled derivatives of the Cystic Fibrosis drug, ivacaftor. (Masters of Science dissertation). Retrieved from Ryerson University Library and Archives Digital Repository. http://digital.library.ryerson.ca/islandora/object/RULA:1478

European Medicines Agency (2012) Assessment report: Kalydeco EMA/473279/2012. http://www.ema.europa.eu/docs/en_GB/document_library/EPAR_-_Public_assessment_report/human/002494/WC500130766.pdf.

Gupta N, Prasad PD, Ghamande S, Moore-Martin P, Herdman AV, Martindale RG, Podolsky R, Mager S, Ganapathy ME and Ganapathy V (2006) Up-regulation of the amino acid transporter ATB(0,+) (SLC6A14) in carcinoma of the cervix. *Gynecol Oncol* **100**(1): 8-13.

Hanrahan JW, Matthes E, Carlile G and Thomas DY (2017) Corrector combination therapies for F508del-CFTR. *Curr Opin Pharmacol* **34**: 105-111.

He L, Aleksandrov AA, Serohijos AW, Hegedus T, Aleksandrov LA, Cui L, Dokholyan NV and Riordan JR (2008) Multiple membrane-cytoplasmic domain contacts in the cystic fibrosis transmembrane conductance regulator (CFTR) mediate regulation of channel gating. *J Biol Chem* **283**(39): 26383-26390.

He L, Kota P, Aleksandrov AA, Cui L, Jensen T, Dokholyan NV and Riordan JR (2013) Correctors of DeltaF508 CFTR restore global conformational maturation without thermally stabilizing the mutant protein. *Faseb j* **27**(2): 536-545.

Hoglund P, Haila S, Socha J, Tomaszewski L, Saarialho-Kere U, Karjalainen-Lindsberg ML, Airola K, Holmberg C, de la Chapelle A and Kere J (1996) Mutations of the Down-regulated in adenoma (DRA) gene cause congenital chloride diarrhoea. *Nat Genet* **14**(3): 316-319.

Jih KY and Hwang TC (2013) Vx-770 potentiates CFTR function by promoting decoupling between the gating cycle and ATP hydrolysis cycle. *Proc Natl Acad Sci U S A* **110**(11): 4404-4409.

Karunakaran S, Ramachandran S, Coothankandaswamy V, Elangovan S, Babu E, Periyasamy-Thandavan S, Gurav A, Gnanaprakasam JP, Singh N, Schoenlein PV, Prasad PD, Thangaraju M and Ganapathy V (2011) SLC6A14 (ATB0,+) protein, a highly

concentrative and broad specific amino acid transporter, is a novel and effective drug target for treatment of estrogen receptor-positive breast cancer. *J Biol Chem* **286**(36): 31830-31838.

Ko SB, Zeng W, Dorwart MR, Luo X, Kim KH, Millen L, Goto H, Naruse S, Soyombo A, Thomas PJ and Muallem S (2004) Gating of CFTR by the STAS domain of SLC26 transporters. *Nat Cell Biol* **6**(4): 343-350.

Kumar A, Chatterjee I, Gujral T, Alakkam A, Coffing H, Anbazhagan AN, Borthakur A, Saksena S, Gill RK, Alrefai WA and Dudeja PK (2017) Activation of Nuclear Factor-kappaB by Tumor Necrosis Factor in Intestinal Epithelial Cells and Mouse Intestinal Epithelia Reduces Expression of the Chloride Transporter SLC26A3. *Gastroenterology* **153**(5): 1338-1350.e1333.

Li J, Xia F and Reithmeier RA (2014a) N-glycosylation and topology of the human SLC26 family of anion transport membrane proteins. *Am J Physiol Cell Physiol* **306**(10): C943-960.

Li W, Soave D, Miller MR, Keenan K, Lin F, Gong J, Chiang T, Stephenson AL, Durie P, Rommens J, Sun L and Strug LJ (2014b) Unraveling the complex genetic model for cystic fibrosis: pleiotropic effects of modifier genes on early cystic fibrosis-related morbidities. *Hum Genet* **133**(2): 151-161.

Loo TW, Bartlett MC and Clarke DM (2008) Processing mutations disrupt interactions between the nucleotide binding and transmembrane domains of P-glycoprotein and the cystic fibrosis transmembrane conductance regulator (CFTR). *J Biol Chem* **283**(42): 28190-28197.

Loo TW, Bartlett MC and Clarke DM (2013) Corrector VX-809 stabilizes the first transmembrane domain of CFTR. *Biochem Pharmacol* **86**(5): 612-619.

Loo TW and Clarke DM (2006) Using a cysteine-less mutant to provide insight into the structure and mechanism of CFTR. *J Physiol* **572**(Pt 2): 312.

Loo TW and Clarke DM (2011) Repair of CFTR folding defects with correctors that function as pharmacological chaperones. *Methods Mol Biol* **741**: 23-37.

Matthes E, Goepp J, Carlile GW, Luo Y, Dejgaard K, Billet A, Robert R, Thomas DY and Hanrahan JW (2016) Low free drug concentration prevents inhibition of F508del CFTR functional expression by the potentiator VX-770 (ivacaftor). *Br J Pharmacol* **173**(3): 459-470.

Mendoza JL, Schmidt A, Li Q, Nuvaga E, Barrett T, Bridges RJ, Feranchak AP, Brautigam CA and Thomas PJ (2012) Requirements for efficient correction of DeltaF508 CFTR revealed by analyses of evolved sequences. *Cell* **148**(1-2): 164-174.

Molinski SV, Ahmadi S, Hung M and Bear CE (2015) Facilitating Structure-Function Studies of CFTR Modulator Sites with Efficiencies in Mutagenesis and Functional Screening. *J Biomol Screen* **20**(10): 1204-1217.

Mount DB and Romero MF (2004) The SLC26 gene family of multifunctional anion exchangers. *Pflugers Arch* **447**(5): 710-721.

Okiyoneda T, Veit G, Dekkers JF, Bagdany M, Soya N, Xu H, Roldan A, Verkman AS, Kurth M, Simon A, Hegedus T, Beekman JM and Lukacs GL (2013) Mechanism-based corrector combination restores DeltaF508-CFTR folding and function. *Nat Chem Biol* **9**(7): 444-454.

Oreopoulos J, Epand RF, Epand RM and Yip CM (2010) Peptide-induced domain formation in supported lipid bilayers: direct evidence by combined atomic force and polarized total internal reflection fluorescence microscopy. *Biophys J* **98**(5): 815-823.

Oreopoulos J and Yip CM (2009) Probing membrane order and topography in supported lipid bilayers by combined polarized total internal reflection fluorescence-atomic force microscopy. *Biophys J* **96**(5): 1970-1984.

Patel HH, Murray F and Insel PA (2008) G-protein-coupled receptor-signaling components in membrane raft and caveolae microdomains. *Handb Exp Pharmacol*(186): 167-184.

Pedemonte N, Sonawane ND, Taddei A, Hu J, Zegarra-Moran O, Suen YF, Robins LI, Dicus CW, Willenbring D, Nantz MH, Kurth MJ, Galietta LJ and Verkman AS (2005) Phenylglycine and sulfonamide correctors of defective delta F508 and G551D cystic fibrosis transmembrane conductance regulator chloride-channel gating. *Mol Pharmacol* **67**(5): 1797-1807.

Rabeh WM, Bossard F, Xu H, Okiyoneda T, Bagdany M, Mulvihill CM, Du K, di Bernardo S, Liu Y, Konermann L, Roldan A and Lukacs GL (2012) Correction of both NBD1 energetics and domain interface is required to restore DeltaF508 CFTR folding and function. *Cell* **148**(1-2): 150-163.

Ren HY, Grove DE, De La Rosa O, Houck SA, Sopha P, Van Goor F, Hoffman BJ and Cyr DM (2013) VX-809 corrects folding defects in cystic fibrosis transmembrane conductance regulator protein through action on membrane-spanning domain 1. *Mol Biol Cell* **24**(19): 3016-3024.

Serohijos AW, Hegedus T, Aleksandrov AA, He L, Cui L, Dokholyan NV and Riordan JR (2008) Phenylalanine-508 mediates a cytoplasmic-membrane domain contact in the

CFTR 3D structure crucial to assembly and channel function. *Proc Natl Acad Sci U S A* **105**(9): 3256-3261.

Simons K and Toomre D (2000) Lipid rafts and signal transduction. *Nat Rev Mol Cell Biol* **1**(1): 31-39.

Steinberg SF (2008) Structural basis of protein kinase C isoform function. *Physiol Rev* **88**(4): 1341-1378.

Strug LJ, Gonska T, He G, Keenan K, Ip W, Boelle PY, Lin F, Panjwani N, Gong J, Li W, Soave D, Xiao B, Tullis E, Rabin H, Parkins MD, Price A, Zuberbuhler PC, Corvol H, Ratjen F, Sun L, Bear CE and Rommens JM (2016) Cystic fibrosis gene modifier SLC26A9 modulates airway response to CFTR-directed therapeutics. *Hum Mol Genet* **25**(20): 4590-4600.

Sun L, Rommens JM, Corvol H, Li W, Li X, Chiang TA, Lin F, Dorfman R, Busson PF, Parekh RV, Zelenika D, Blackman SM, Corey M, Doshi VK, Henderson L, Naughton KM, O'Neal WK, Pace RG, Stonebraker JR, Wood SD, Wright FA, Zielenski J, Clement A, Drumm ML, Boelle PY, Cutting GR, Knowles MR, Durie PR and Strug LJ (2012) Multiple apical plasma membrane constituents are associated with susceptibility to meconium ileus in individuals with cystic fibrosis. *Nat Genet* **44**(5): 562-569.

Trittler R and Hug M (2014) PKP-017 Monitoring of ivacaftor serum levels. *European Journal of Hospital Pharmacy: Science and Practice* **21**(Suppl 1): A143-A144.

Van Goor F, Hadida S, Grootenhuis PD, Burton B, Cao D, Neuberger T, Turnbull A, Singh A, Joubran J, Hazlewood A, Zhou J, McCartney J, Arumugam V, Decker C, Yang J, Young C, Olson ER, Wine JJ, Frizzell RA, Ashlock M and Negulescu P (2009) Rescue of CF

airway epithelial cell function in vitro by a CFTR potentiator, VX-770. *Proc Natl Acad Sci U S A* **106**(44): 18825-18830.

Van Goor F, Hadida S, Grootenhuis PD, Burton B, Stack JH, Straley KS, Decker CJ, Miller M, McCartney J, Olson ER, Wine JJ, Frizzell RA, Ashlock M and Negulescu PA (2011) Correction of the F508del-CFTR protein processing defect in vitro by the investigational drug VX-809. *Proc Natl Acad Sci U S A* **108**(46): 18843-18848.

Veit G, Avramescu RG, Perdomo D, Phuan PW, Bagdany M, Apaja PM, Borot F, Szollosi D, Wu YS, Finkbeiner WE, Hegedus T, Verkman AS and Lukacs GL (2014) Some gating potentiators, including VX-770, diminish DeltaF508-CFTR functional expression. *Sci Transl Med* **6**(246): 246ra297.

Vertex Pharmaceuticals Incorporated (2017) Highlights of prescribing information. https://pi.vrtx.com/files/uspi_ivacaftor.pdf

Walsh P, Vanderlee G, Yau J, Campeau J, Sim VL, Yip CM and Sharpe S (2014) The mechanism of membrane disruption by cytotoxic amyloid oligomers formed by prion protein(106-126) is dependent on bilayer composition. *J Biol Chem* **289**(15): 10419-10430.

Wang Y, Loo TW, Bartlett MC and Clarke DM (2007) Correctors promote maturation of cystic fibrosis transmembrane conductance regulator (CFTR)-processing mutants by binding to the protein. *J Biol Chem* **282**(46): 33247-33251.

Xu J, Henriksnas J, Barone S, Witte D, Shull GE, Forte JG, Holm L and Soleimani M (2005) SLC26A9 is expressed in gastric surface epithelial cells, mediates Cl-/HCO3- exchange, and is inhibited by NH4+. *Am J Physiol Cell Physiol* **289**(2): C493-505.

FOOTNOTES

This work was supported by Cystic Fibrosis Canada; CIHR [Grants MOP-97954, GPG-102171]; and NSERC [Grant RGPIN-2015-043].

FIGURE LEGENDS

Figure 1. Supra-pharmacological concentration of VX-770 destabilizes protein expression of VX-809 rescued F508del-CFTR. (A) Immunoblot of F508del-CFTR treated with 3 μM VX-809 and 0, 0.1 and 10 μM VX-770 at 37°C for 48 h with no VX-809 treatment as control and calnexin (CNX) as loading control. **(B)** Densitometry analysis of immunoblots of band *C* abundance normalized to calnexin (CNX) loading control and DMSO treatment shows that chronic treatment with 10 μM VX-770, and not 0.1 μM VX-770, significantly decreased band *C* abundance relative to VX-809 rescue of F508del-CFTR to a similar level as no VX-809 rescue (n = 5 for all conditions). Results are presented as mean ± SD and analyzed by One-way ANOVA and Dunnett's post-hoc test (**$p < 0.01$ and ***$p < 0.001$ compared to vehicle). **(C)** Densitometry analysis of immunoblots of band *B* abundance normalized to calnexin (CNX) loading control and DMSO treatment shows that chronic treatment with 10 μM VX-770, and not 0.1 μM VX-770, also significantly decreased band *B* abundance relative to VX-809 rescue of F508del-CFTR (n = 5 for all conditions). Results are presented as mean ± SD and analyzed by One-way ANOVA and Dunnett's post-hoc test (**$p < 0.01$ compared to vehicle).

Figure 2. Supra-pharmacological concentration of VX-770 abolishes VX-809 rescue effect at the ICL4: NBD1 interface of cys-less variant of F508del-CFTR. (A) Immunoblot of deglycosylation studies of V510C/A1067C cys-less variants of Wt- and F508del-CFTR without (-) and with (+) BMOE treatment. *V510C/A1067C cys-less variant of Wt-CFTR (-) BMOE:* No

Molecular Pharmacology Fast Forward. Published on June 14, 2018 as DOI: 10.1124/mol.118.112177
This article has not been copyedited and formatted. The final version may differ from this version.

glycanase (-) treatment resulted in band *C* and *B*. Endoglycosidase H (H) treatment resulted in band *C* and band *A*. PNGase F (F) treatment resulted in band *A*. *V510C/A1067C cys-less variant of Wt-CFTR (+) BMOE:* No glycanase (-) treatment resulted in cross-linked band *C* (ǂ), population containing band *C* and cross-linked band *B* (C✻), and band *B*. Endoglycosidase H (H) treatment resulted in cross-linked band *C* (ǂ), population of band *C* and cross-linked band *A* (C△), and band *A*. PNGase F (F) treatment resulted in cross-linked band *A* (△) and band *A*. *V510C/A1067C cys-less variant of F508del-CFTR (-) BMOE:* No glycanase (-) treatment resulted in band *B*, Endoglycosidase H (H) treatment resulted in band *A* and PNGase F (F) treatment resulted in band *A*. *V510C/A1067C cys-less variant of F508del-CFTR (+) BMOE:* No glycanase (-) treatment resulted in cross-linked band *B* (✻) and band *B*. Endoglycosidase H (H) treatment resulted in cross-linked band *A* (△) and band *A*. PNGase F (F) treatment resulted in cross-linked band *A* (△) and band *A*. **(B)** Immunoblot of V510C/A1067C cys-less variant of F508del-CFTR pre-treated with vehicle (DMSO, 0.1%), VX-809 (3 μM), VX-770 (100 nM or 10 μM), or combination of VX-809 and (+) VX-770 (100 nM VX-770 or 10 μM) at 27°C for 24 h. **(C)** Densitometry results of normalized cross (X)-linked band *B* (✻) to band *B* show that VX-809 significantly increased the abundance of relative X-linked band *B* (✻) and this effect was abolished upon additional treatment with 10 μM VX-770 but not with 100 nM VX-770 (n = 6 for DMSO and VX-809 + 100 nM VX-770 conditions; n = 7 for VX-809, 100 nM VX-770 and 10 μM VX-770 conditions; and n = 8 for

VX-809 + 10 μM VX-770 condition). Results are presented as mean ± SD and analyzed by One-way ANOVA and Dunnett's post-hoc test (*$p < 0.05$ compared to vehicle).

Figure 3. VX-770 exerts destabilizing effect on membrane proteins of the solute carrier (SLC) family. (i) Representative immunoblots of **(A)** SLC26A3, **(B)** SLC26A9, and **(C)** SLC6A14 show different glycosylation forms of the proteins as previously reported (Li et al., 2014a). SLC proteins were treated with 0, 0.1, 1, 2 and 10 μM of VX-770 at 27°C for 24 h with actin as loading control. **(ii)** Densitometry analyses of total protein relative to DMSO treatment and actin loading control of **(A)** SLC26A3 (n = 4 for all conditions), **(B)** SLC26A9 (n = 5 for all conditions), and **(C)** SLC6A14 (n = 4 for all conditions). SLC26A3 expression significantly decreased after 0.1 μM VX-770, SLC26A9 expression significantly decreased after 2 μM VX-770, and SLC6A14 expression significantly decreased after 10 μM VX-770. Results are presented as mean ± SD and analyzed by One-way ANOVA and Dunnett's post-hoc test (*$p < 0.05$, **$p < 0.01$, and ***$p < 0.001$ compared to vehicle).

Figure 4. Lipophilicity of VX-770 may correlate with its destabilizing effect on F508del-CFTR. (A) Immunoblots of F508del-CFTR from HEK-293 overexpressing F508del-CFTR cells chronically treated with VX-770 and its derivatives at 0.1 μM or 10 μM at 27°C for 24 h compared to DMSO as a negative control. Calnexin (CNX) was used as a loading control. **(B)** Correlation plot of the lipophilicity measure also known as log*P* and the abundance of cell surface band *C* relative to band *C* and band *B* (*C*+*B*) of F508del-CFTR treated with 10 μM of VX-770 and its derivatives at 27°C for 24 h. There was a significant correlation suggesting that the higher the

lipophilicity of the drug derivative may correlate to less cell surface expression of F508del-CFTR (n = 4 for all derivatives). Results were analyzed by linear regression and Spearman's correlation (r = -0.69 and *p < 0.05). **(C)** Comparisons of band *C* relative to band *C* and band *B* (*C*+*B*) of F508del-CFTR chronically treated with DMSO, 10 μM VX-770 and 10 μM SE-03 at 27°C for 24 h. Densitometry analyses show that treatment with 10 μM VX-770 significantly decreased band *C* relative to band *C*+*B* of F508del-CFTR whereas treatment with 10 μM SE-03 did not compared to DMSO (n = 5 for all conditions). Results are presented as mean ± SD and analyzed by One-way ANOVA and Dunnett's post-hoc test (**p < 0.01 compared to vehicle). **(D)** FLiPR channel function studies of VX-809 rescued F508del-CFTR stimulated (Stim.) with vehicle (labeled as "a"), 1 μM cAMP agonist, forskolin (Fsk) (labeled as "b"), 1 μM Fsk and 10 μM VX-770 (labeled as "c"), or 1 μM Fsk and 10 μM SE-03 (labeled as "d"), and then inhibited with $CFTR_{inh}$-172. *Inset*: Immunoblot of F508del-CFTR after the FLiPR assay shows that the level of band *C* in each condition were relatively similar compared to calnexin (CNX) as a loading control. **(E)** Quantification of the maximum peak of Fsk stimulation in the FLiPR assay relative to baseline and DMSO show that acute treatment with 10 μM VX-770 and 10 μM SE-03 with 1 μM Fsk significantly potentiated CFTR chloride flux compared to 1 μM Fsk alone (DMSO, n = 3 for all conditions, average of 8 wells per replicate). Results are presented as mean ± SD and analyzed by One-way ANOVA and Dunnett's post-hoc test (*p < 0.05 and **p < 0.01 compared to 1 μM Fsk).

Figure 5. Supra-pharmacological concentration of VX-770 appears to increase membrane fluidity and reorganize the bilayer. Representative pTIRF images of a 30 x 30 μm section of a DOPC/bSM/cholesterol lipid raft-like model prior to addition of **(A)** 10 μM VX-770 and **(C)** 10 μM SE-03. pTIRF images at 1 h incubation with **(B)** 10 μM VX-770 and **(D)** 10 μM SE-03. First

row represents the pTIRF images obtained by substrate parallel excitation (F_s) and the second row represents the pTIRF images obtained by perpendicular excitation (F_p) of the DiI-C_{18} fluorescent dye. Third row represents the same images coloured by the order parameter $<P_2>$. The last row represents the histogram summarizing the range of $<P_2>$ with the mean value and margin of error indicated at the bottom. Two bilayers were studied per condition with 3-6 fields analyzed per bilayer.

Molecular Pharmacology Fast Forward. Published on June 14, 2018 as DOI: 10.1124/mol.118.112177
This article has not been copyedited and formatted. The final version may differ from this version.

Figure 1

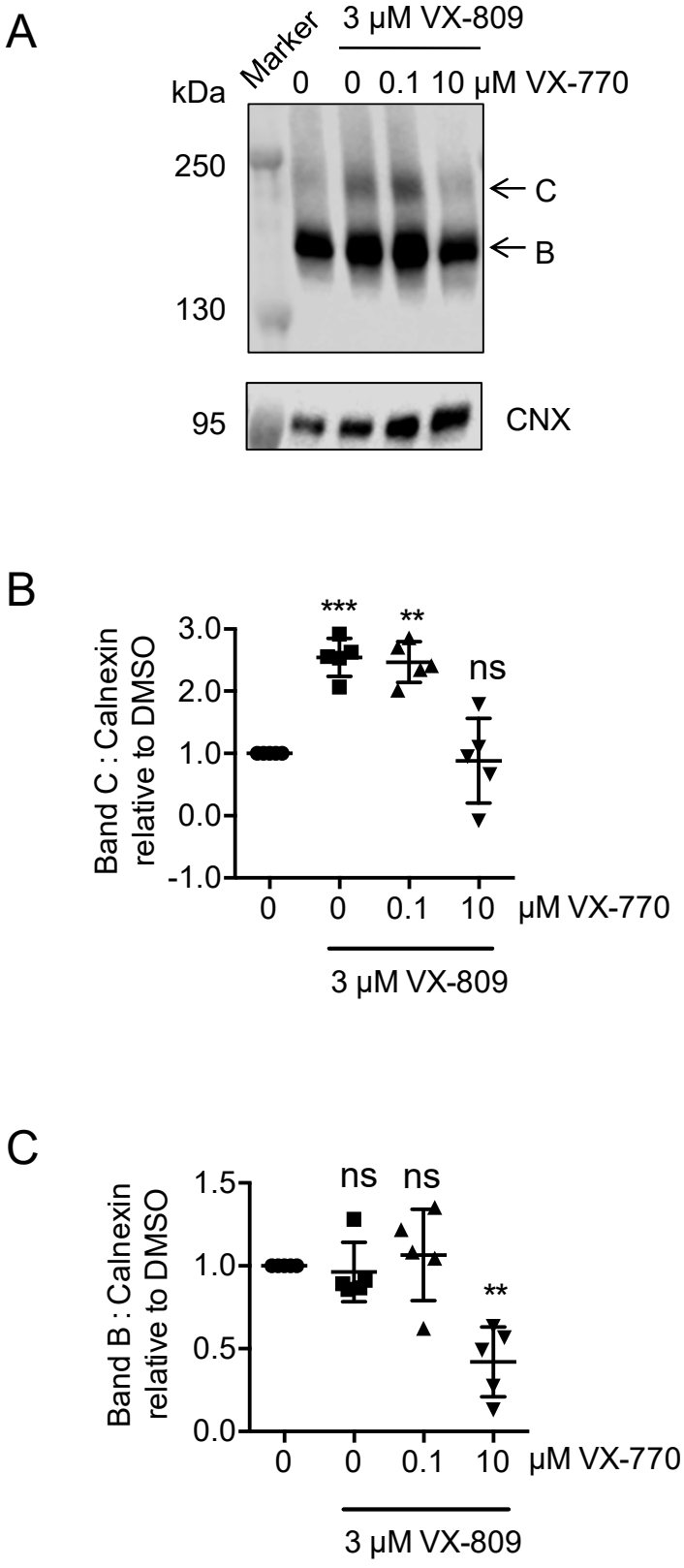

Molecular Pharmacology Fast Forward. Published on June 14, 2018 as DOI: 10.1124/mol.118.112177
This article has not been copyedited and formatted. The final version may differ from this version.

Figure 2

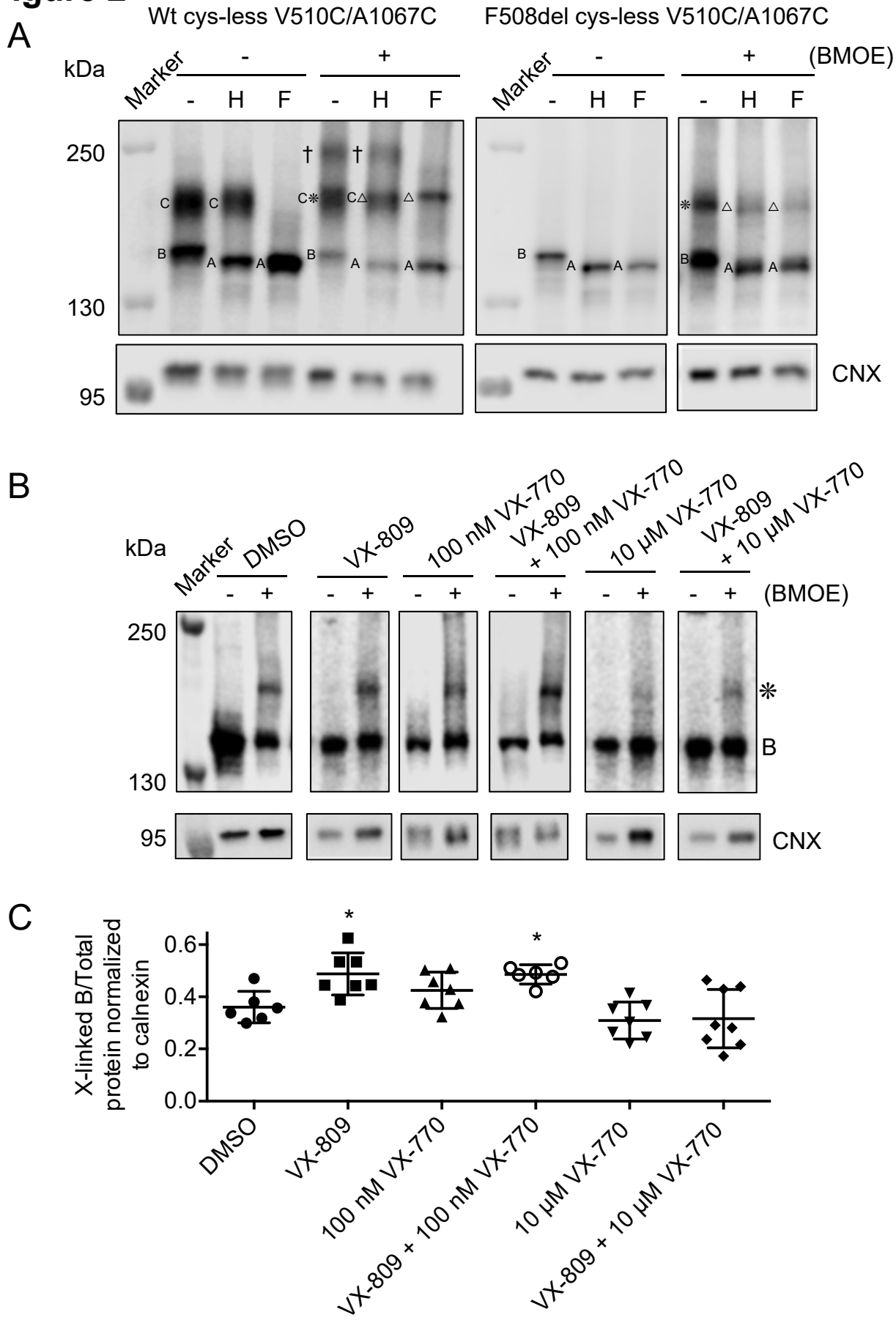

Molecular Pharmacology Fast Forward. Published on June 14, 2018 as DOI: 10.1124/mol.118.112177
This article has not been copyedited and formatted. The final version may differ from this version.

Figure 3

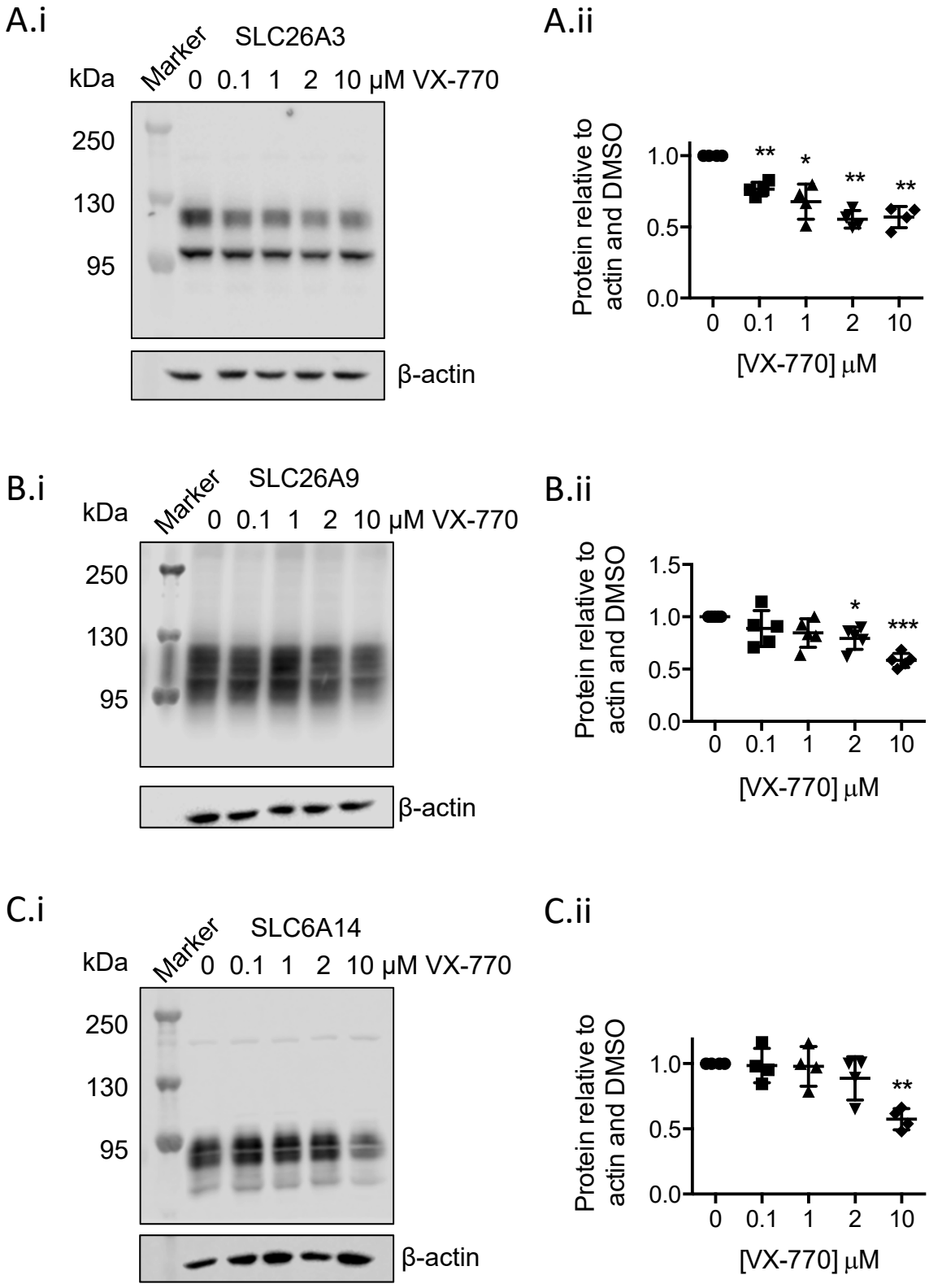

Molecular Pharmacology Fast Forward. Published on June 14, 2018 as DOI: 10.1124/mol.118.112177
This article has not been copyedited and formatted. The final version may differ from this version.

Figure 4

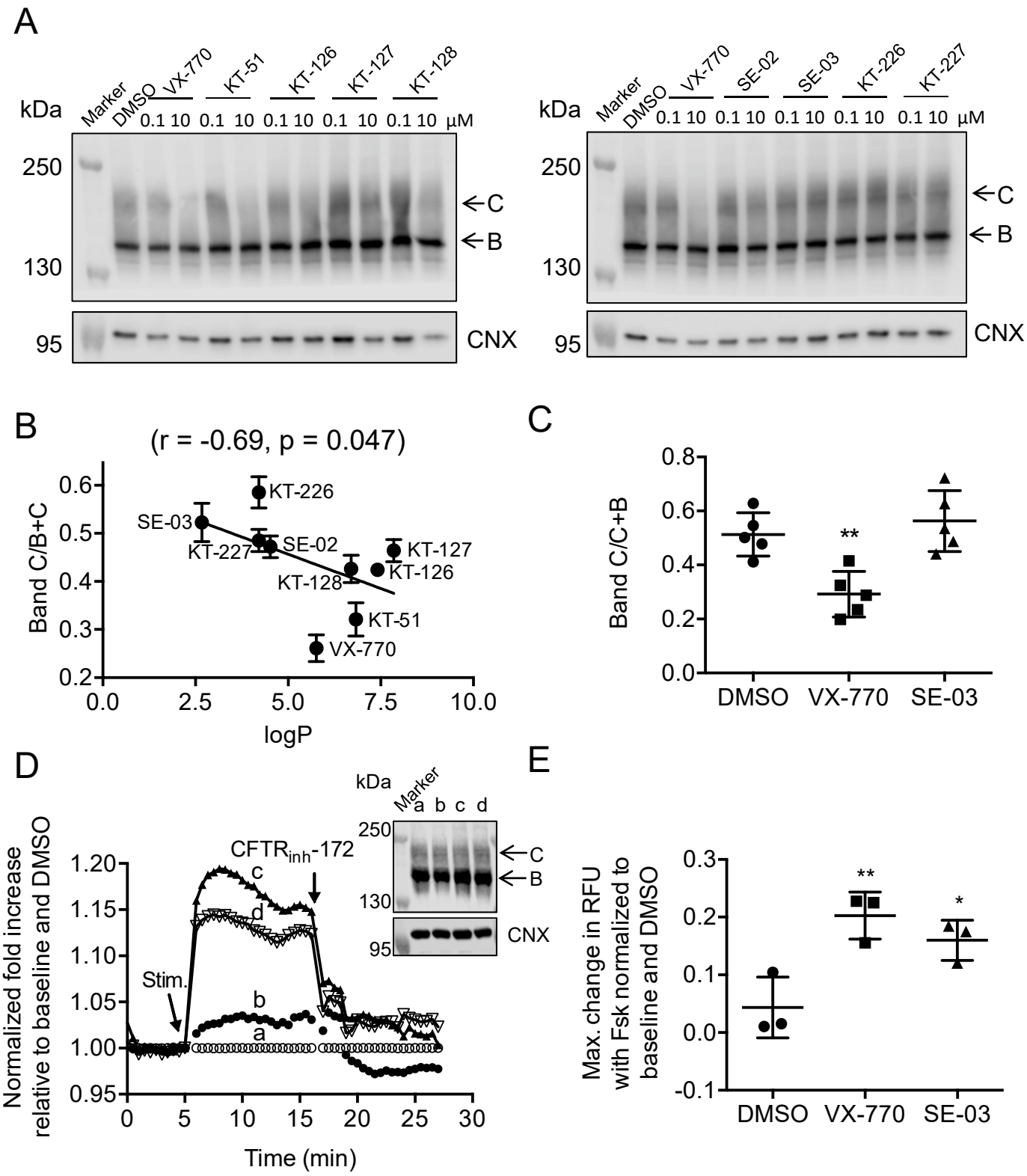

Molecular Pharmacology Fast Forward. Published on June 14, 2018 as DOI: 10.1124/mol.118.112177
This article has not been copyedited and formatted. The final version may differ from this version.

Figure 5